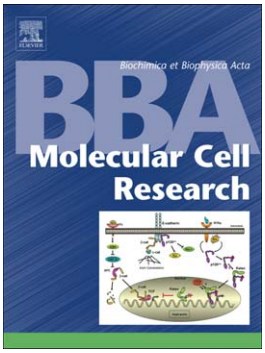

8-Dehydrosterols induce membrane traffic and autophagy defects through V-ATPase dysfunction in *Saccharomyces cerevisae*

Agustín Hernández, Gloria Serrano-Bueno, José Román Perez-Castiñeira, Aurelio Serrano

PII: S0167-4889(15)00294-3
DOI: doi: 10.1016/j.bbamcr.2015.09.001
Reference: BBAMCR 17654

To appear in: *BBA - Molecular Cell Research*

Received date: 27 July 2015
Accepted date: 1 September 2015

Please cite this article as: Agustín Hernández, Gloria Serrano-Bueno, José Román Perez-Castiñeira, Aurelio Serrano, 8-Dehydrosterols induce membrane traffic and autophagy defects through V-ATPase dysfunction in *Saccharomyces cerevisae*, *BBA - Molecular Cell Research* (2015), doi: 10.1016/j.bbamcr.2015.09.001

8-Dehydrosterols induce membrane traffic and autophagy defects through V-ATPase dysfunction in *Saccharomyces cerevisae*

Authors:
Agustín Hernández*, Gloria Serrano-Bueno, José Román Perez-Castiñeira, Aurelio Serrano*

Affiliation:
Instituto de Bioquímica Vegetal y Fotosíntesis, Universidad de Sevilla–CSIC, Avda Américo Vespucio 48, 41092 Sevilla, Spain

*Corresponding authors. Telephone: +34 954 489500, Fax: +34 954 460065, E-mails: agustin.hernandez@ibvf.csic.es (AH) and aurelio@ibvf.csic.es (AS). Please, all communications with Editorial and Production offices to be done through AH.

Running title: Endocytosis and autophagy in *erg2Δ* mutants

Keywords: V-ATPase, H^+-pumping pyrophosphatase, abnormal sterols, vacuole, autophagy, endocytosis.

Abbreviations: GFP: green fluorescent protein, LY: Lucifer Yellow, PPi: inorganic pyrophosphate, H^+-PPase: H^+-pumping pyrophosphatase; PPase: inorganic pyrophosphatase, UPR: unfolded protein response, PI: propidium iodide, IP: immunoprecipitation.

Abstract

8-dehydrosterols are present in a wide range of biologically relevant situations, from human rare diseases to amine fungicide-treated fungi and crops. However, the molecular bases of their toxicity are still obscure. We show here that 8-dehydrosterols, but not other sterols, affect yeast vacuole acidification through V-ATPases. Moreover, *erg2Δ* cells display reductions in proton pumping rates consistent with ion-transport uncoupling *in vitro*. Concomitantly, subunit Vph1p shows conformational changes in the presence of 8-dehydrosterols. Expression of the plant vacuolar H^+-pumping pyrophosphatase as an alternative H^+-pump relieves Vma^--like phenotypes in *erg2Δ*-derived mutant cells. As a consequence of these acidification defects, endo- and exocytic traffic deficiencies that can be alleviated with a H^+-pumping pyrophosphatase are also observed. Despite their effect on membrane traffic, 8-dehydrosterols do not induce endoplasmic reticulum stress or assembly defects on the V-ATPase. Autophagy is a V-ATPase dependent process and *erg2Δ* mutants accumulate autophagic bodies under nitrogen starvation similar to Vma^- mutants. In contrast to classical Atg^- mutants, this defect is not accompanied by impairment of traffic through the CVT pathway, processing of Pho8Δ60p, GFP-Atg8p localisation or difficulties to survive under nitrogen starvation conditions, but it is concomitant to reduced vacuolar protease activity. All in all, *erg2Δ* cells are autophagy mutants albeit some of their phenotypic features differ from classical Atg^- defective cells. These results may pave the way to understand the etiology of sterol-related diseases, the cytotoxic effect of amine fungicides, and may explain the tolerance to these compounds observed in plants.

1. Introduction

In eukaryotes, proper acidification of organellar lumina is a paramount process that influences vesicle fusion [1, 2], transport of cargoes and membranes [3] or storage of metabolites like amino acids [4], among other processes. At the cellular level, manipulation of the proteins responsible for the generation and maintenance of proton gradients across organellar membranes has been proved to affect autophagy [5], alter resistance to some abiotic stresses in plants [6, 7] and represents an attractive target for cell death induction in cancer therapy [8]. Plants, microalgae and many protists display a double set of primary H^+-pumps in intracellular organelles: in addition to V-ATPases, they present membrane-bound H^+-pumping pyrophosphatases (H^+-PPases) [9-11]. These simpler H^+ pumps are also related to a radical difference on cytosolic inorganic pyrophosphate (PPi) removal: plants and microalgae couple PPi hydrolysis to ion transport by membrane-bound H^+-PPases, while fungi and animals rely on soluble PPases that dissipate PPi energy as heat [10, 11]. The significance of this double set of pumps in intracellular organelles is still an unresolved question, as much as its influence on anabolism through regulation of PPi levels.

Sterols are one of the main components of lipid bilayers and play a decisive role in determining membrane-associated processes like cell signalling and membrane-bound enzyme activity. It is not surprising then that several genetic diseases have been described to be caused by mutations in key enzymes in human sterol biosynthesis, such as X-chromosome linked chondrodysplasia punctata (CDPX2) [12]. This condition is associated to mutations in the gene *EBP* encoding the human 3β-hydroxysteroid-Δ^8,Δ^7-isomerase [13]. Although there is a vivid interest in rare diseases, the biochemical or cellular mechanisms of CDPX2 are still unknown. On the other hand, amine fungicides are effective inhibitors that target sterol-Δ^8,Δ^7-isomerase and sterol-Δ^{14}-reductase. Paradoxically, plants and fungi have been known for a long time to display similar *in vitro* inhibitor sensitivity in their sterol biosynthetic enzymes [14], but the latter organisms are far more sensitive to inhibition of this pathway. So far, no cellular explanation for this phenomenon is available. Furthermore, plant sterol metabolism is receiving increasing attention, among other reasons because fungicides targeting ergosterol biosynthesis, although well tolerated, are known to disturb plant development [15, 16] and, more recently, they have been observed to affect photosynthesis [17].

The *Saccharomyces cerevisiae ERG2* gene encodes the yeast sterol-Δ^8,Δ^7-isomerase, an orthologue of human EBP and *Arabidopsis thaliana* HYD1 [18]. Noticeably, mutants defective in *ERG2* are known to accumulate 8-dehydrosterols [19] and to display a series of phenotypes akin to those observed in V-ATPase mutants [20-22], and they were early identified as endocytic traffic mutant *end11* [23]. Defects leading to the accumulation of some abnormal sterols, namely 14α-methylated sterol precursors, were reported to affect V-ATPase [24, 25] and proposed as part of the fungicidal effect of azole antifungals, but the effect of 8-dehydrosterols is still unknown.

In this report, we show that 8-dehydrosterols affect V-ATPase function. Consequently, some of the phenotypes related to the presence of 8-dehydrosterols in yeast membranes, such as inability to grow at alkaline pH or in the presence of Zn^{2+} and defects in endo- and exocytosis, are alleviated in the presence of a plant H^+-PPase as an alternative proton pump. Also, we show that *erg2Δ* cells display defects in autophagy that can be rescued by a H^+-PPase. These results can help to understand the cellular effects of 8-dehydrosterols, the significance of the presence of a double set of H^+-pumps in endomembrane systems of plants and many eukaryotic microorganisms and help to understand their natural resistance to commonly used inhibitors of sterol biosynthesis.

2. Experimental procedures

2.1 Yeast strains, plasmids and growth conditions

All strains are derivatives of *Saccharomyces cerevisiae* strain W303-1a (MATa *leu2-3,112 trp1-1 can1-100 ura3-1 ade2-1 his3-11,15*) or SE6210 (*MATα leu2-3,112 ura3-52 his3-Δ200 trp1-Δ901 suc2-Δ9 lys2-801*). Relevant genotypes are described on **Table 1**. Yeast soluble PPase *IPP1* or TcGFP-AVP1, a chimaera consisting of the H^+-PPase vacuolar isoform AVP1 from *Arabidopsis thaliana* fused to the *N*-terminal sequence of the H^+-PPase TcVP from the protist *Tripanosoma cruzi* and the sequence of the green fluorescent protein from *Aequorea victoria*, were expressed from a pRS699 multicopy plasmid as described [26]. Introduction of plasmids into yeast cells was done by the lithium-acetate method [27]. Cells were routinely grown on standard YP or synthetic media supplemented with appropriate carbon sources [28]. Unless otherwise stated, all determinations were done on exponentially-growing cells ($0.5 < A_{600} > 0.8$). For drop tests, cells were grown to early stationary phase. A_{600} of cultures were then adjusted to 0.4 (*ca* $4x10^6$ cells/ml) with water and three 10-fold serial dilutions in water prepared from them. Two-point-five microliter aliquots from each dilution were placed onto appropriate agar plates, resulting in *ca* 10^4, 10^3, 10^2 or 10 cells per spot, accordingly. For analysis of responses under nitrogen starvation, cells were incubated in nitrogen starvation minimal medium (0.17% yeast nitrogen base without amino acids and ammonium sulphate supplemented with 2% glucose) for three hours prior analysis, except in the case of accumulation of autophagic bodies, when incubation time was five hours.

2.2 Whole cell and membrane preparations for immunochemical and enzymatic assays

For whole cell extracts, yeast cells were washed, resuspended in Thorner buffer without β-mercaptoethanol (8 M urea, 10% SDS, 40 mM Tris, pH 6.8) and subjected to vigorous vortexing for five one-min bursts in the presence of glass beads (0.5 mm Ø). Cell debris and glass beads were collected by centrifugation at 16,000 x *g* for 10 min. The supernatant constituted the whole cell extract.

Total membranes were isolated by differential centrifugation. Briefly, yeast cells were washed, resuspended in 25 mM Tris-HCl pH 8.0, 2 mM EDTA, 2 mM DTT and protease inhibitors (Sigma, St. Louis, MO) and subjected to ten 30 s vortexing bursts with 1 min resting periods on ice. Glass beads and debris were precipitated at 3000 x g for 5 min and the resulting supernatant was centrifuged at 50,000 x g for 30 min. The pellet constituted the total membrane fraction.

For vacuolar vesicles, intact vacuoles were isolated essentially as described [29] with the only modification of using a single 8% ficoll gradient. Vacuoles were vesiculated by resuspension in TKE buffer (10 mM Tris/HCl pH 7.5, 2 mM KCl, 1 mM EDTA and protease inhibitors); vesicles were recovered after centrifugation at 100,000 x *g* for 30 min and resuspension in TKE. The formation of a ΔpH was evaluated as the ACMA fluorescence quenching produced by the activity of the tonoplast H^+-ATPase using the following reaction mixture: 1 μM ACMA, 20 mM MOPS-Tris pH 7.2, 25 mM KCl, 2 mM $MgCl_2$, and vacuolar membrane preparation (up to 50 μg of protein). The assay was initiated with the addition of 1.5 mM ATP. Recovery of fluorescence, as a proof of gradient formation, was induced by adding 3 μM gramicidin D. ATPase hydrolytic activities were assayed as described [30].

2.3 Microscopic techniques

Cells were visualized using a Leica DM 6000B epifluorescence microscope with either Nomarsky optics, Texas red or FITC fluorescence filters, as appropriate. Endocytosis was followed by vital staining using the red fluorescent vital dye FM4-64 (Invitrogen, Carlsbad, CA): yeast strains were grown to mid-log phase and later pulse-labelled with FM4-64 for 30 min on ice, washed and chased for 60 additional min to display intracellular compartments as described in [31]. Additionally, Lucifer Yellow dye (Sigma-Aldrich, Madrid) was used to reveal fluid phase endocytosis [32]. Cell counting was done over Nomarsky optics (autophagic bodies) or fluorescence pictures (LY); a minimum of 300 cells were counted per experiment. Data presented are average ± SE of three independent experiments.

2.4 Immunoprecipitation assays

For immunoprecipitation assays, cells were grown in 50 ml of culture medium to mid-log phase and washed once in SPMB buffer (1 M sorbitol, 50 mM potassium phosphate buffer pH 7.5, 1 mM $MgCl_2$). Protoplasts were produced by incubation of cells in SPMB using lyticase (5000 units) at 30^{o}C with gentle rocking for 60 min. Protoplasts were centrifuged at 3000 x *g* for 7 min and washed once in YPD *plus* 1.2M sorbitol prior to incubate them in this same medium for 30 min at 30^{o}C. After this, protoplasts were centrifuged at 3000 x *g* for 7 min and washed once in SMPB. After a second centrifugation, the pellet was resuspended in cold IP buffer (PBS supplemented with 1% β-dodecylmaltoside, 1 mM EDTA, 1 mM PMSF, 1 mM benzamidine and a protease inhibitor cocktail (Sigma, St Louis, MO). Cells were solubilized for 30 min on ice and insoluble material was eliminated by centrifugation at 16,000 x *g* for 20 min. The supernatant represented the whole cell extract. Immunoprecipitations were set by adding cell extracts (100 µg of protein) to Protein G-Dynabeads (Invitrogen, Carlsbad, CA) previously bound to 5 µg of anti-Vma1p antibodies in a total volume of 500 µl of PBS *plus* 1% β-dodecylmaltoside. This mixture was incubated overnight at 4^{o}C with mild agitation by tumbling. The following day, the Dynabeads were magnetoprecipitated and washed 5 times with PBS+0.1% β-dodecylmaltoside. Washed pellets were resuspended in Thorner buffer and heated to 95^{o}C for 10 min prior to loading onto SDS-PAGE gels.

2.5 β-Galactosidase assays

ER-stress was measured as the induction of expression of β-galactosidase driven from a fusion of four unfolded protein response promoter elements (4 x UPRE) localised on plasmid pJC104, using *o*-nitrophenyl-β-galactopyranoside as a substrate (Cox and Walter, 1996). Overnight cultures, in triplicate tubes, were diluted and left to grow for 2 generations; after this time, when appropriate, cultures were exposed to stress for 5 h, harvested, and the pellets flash-frozen in liquid nitrogen. Activity of β-galactosidase was measured as in (Giacomini *et al.*, 1992) using SDS and chloroform as permeabilising agents. Total activity, in Miller units, was referred to that found in untreated W303-1a cells.

2.6 Invertase exocytosis

Suc2p-exocytosis was determined as described in [33]. Briefly, cells were grown on 5% glucose YPD to *ca* 8 x 10^6 cells/ml, harvested by centrifugation and resuspended on 0.1% glucose YPD medium. At the indicated times, aliquots of 3.5 x 10^6 cells were taken, centrifuged and metabolism halted by resuspension in 0.5 ml of ice-cold 10 mM azide. Half of this volume was used without further treatment to determine periplasmic invertase activity. The remaining cells were centrifuged, resuspended in 1% Triton X-100, 10 mM azide and subjected to freeze-thawing in liquid nitrogen to permeabilise cells (total invertase activity). Assays to determine invertase activity in samples were done as in [34].

2.7 Other Enzymatic assays

PHO8Δ60 strains were generated by genetic recombination of linear DNA PCR products obtained as described by [35] and are listed in Table 1. Alkaline phosphatase assays were done by quantitation of fluorescence using yeast whole cell extracts and α-naphthyl phosphate as substrate [35].
Protease A activity was determined as described by Jones [36] using haemoglobin as a substrate.

2.8 Protein determination and Western blotting

Protein determination was done using a dye-binding based assay from Bio-Rad (Hercules, CA), according to manufacturer instructions or a modified Lowry assay (Thermo Scientific, Rockford, IL), and using ovoalbumin as a standard. Proteins were separated in SDS-PAGE gels using standard procedures [37]. Proteins were then transferred to nitrocellulose filters and probed with antibodies raised against Vma1p and Vph1p (monoclonals 8B1 and 10D7, respectively; Molecular Probes, Leiden). Proteins were visualised on X-ray films using horseradish peroxidase-coupled secondary antibodies and a chemiluminescence kit (Millipore, Madrid). For trypsin sensitivity assays, 37.5 µg of vacuole membrane vesicle proteins were diluted in PBS to a final volume of 75 µl and incubated at 37 ^{o}C for the duration of the assay. At the beginning of the experiment, 22.5 µg of trypsin were added. At the indicated times, 10 µl aliquots were taken, diluted in electrophoresis loading buffer supplemented with 1 mM PMSF and a protease inhibitor cocktail (Sigma-Aldrich, Madrid), and snap frozen in liquid nitrogen until use. Preliminary experiments indicated no degradation by endogenous proteases in the time-lapse used for these experiments (data not shown). *Western* blot analysis was done as above. Levels of Vph1p were visualised by immunodetection with anti-Vph1p antibodies and quantitation of the chemiluminescent signal was done using a CCD camera and QuantityOne software (BioRad, Madrid). Protein load on gels was quantitated from images obtained using trichloroethanol-enhanced protein tryptophan fluorescence (TETF) [38].

2.9 Survival assays

Yeast strains were transformed with pRS31X series plasmids to complement all auxotrophies not covered by expression plasmids. Cells were grown overnight in glucose-supplemented synthetic medium without appropriate amino acids, next morning cells were washed with sterile distilled water, diluted to A_{600}= 1 and left for the duration of the experiment in nitrogen starvation synthetic medium (0.15% yeast nitrogen base without amino acids and ammonium sulphate) supplemented with 2% glucose. Aliquots were taken at the indicated times and diluted to plate *ca* 300 cells per YPD Petri dish. Actual cell concentrations in the cultures were estimated by counting cells on a hemocytometer. Colonies formed on plates were counted three days after inoculation. Three plates were inoculated per time point and experiment. Data presented are the average ± SE of three independent experiments.

2.10 Other methods

Statistical analysis was done using unpaired *t*-tests with a confidence limit of p=0.05 for significance. Unless otherwise stated, experiments were repeated three times.

3. Results

3.1 A plant H^+-PPase complements erg2Δ phenotypes in yeast

In a recent report, our group described the construction of a chimaeric transporter protein consisting (*N* to *C* termini) of the *N*-terminal signal sequence of the H^+-PPase from *Tripanosoma cruzi* (TcVP) followed by the full amino acid coding sequences of the green fluorescent protein from *Aequorea victoria* and that of the *Arabidopsis thaliana* vacuolar H^+-PPase (AVP1) [39]. This construct is named hereafter TcGFP-AVP1. In a subsequent report we also demonstrated that the TcGFP-AVP1 construct could complement defects in Vma^- yeast mutants due to its capability to acidify intracellular organelles [26]. On Figure 1A we show that this system is well suited to study phenotypes associated to defects in vacuolar acidification. Yeast deletion mutants on the Golgi-

located isoform (*stv1Δ*, SAH5 strain) and on its vacuolar counterpart (*vph1Δ*, SAH6 strain) of the V-ATPase a subunit were constructed as derivatives of YPC3 strain [39]. This genetic background is necessary since absence of the cytosolic soluble PPase Ipp1p is required for heterologous H^+-PPases to pump protons efficiently across endomembrane systems [26]. In particular, this strain has its genomic copy of the essential gene *IPP1* encoding the yeast soluble pyrophosphatase modified to be expressed under the control of the GAL1 promotor; thus, on glucose media its proliferation depends on the activity of an alternative pyrophosphatase expressed from a plasmid. Yeast *vph1Δ* mutants (SAH6) clearly showed that their sensitivity to alkaline pH and zinc, two well-known phenotypic features associated to dysfunction of vacuolar acidification [20, 40], could be reverted by the expression of TcGFP-AVP1 when using glucose as a carbon source. In contrast, *stv1Δ* (SAH5) showed no growth defects on alkaline media or in the presence of zinc (Fig. 1A). Genetic defects in the last steps of ergosterol biosynthesis yield strains that show similar growth phenotypes to those found in Vma^- mutants. To ascertain if these *erg2Δ*-associated phenotypes could be related to a deficiency in vacuolar acidification, we tested the ability of TcGFP-AVP1 to complement the same growth phenotypes tested on *vph1Δ* mutants (Fig. 1B) using a YPC3-derivative where the genomic *ERG2* gene had been deleted by homologous recombination (SAH2 strain). Indeed, heterologous expression of the alternative proton pump TcGFP-AVP1 alleviated the sensitivity to both alkaline medium and zinc in these cells, while overexpression of the control yeast soluble PPase *IPP1* did not.

We wanted to confirm that the acidification defects were also part of the set of effects induced by amine fungicides. Indeed, well tolerated concentrations of Zn^{2+} (2 mM) became growth impairing to a wild-type yeast strain in the presence of sub-lethal concentrations of tridemorph (1 µM) (Fig. 1C), an amine fungicide that specifically inhibits Erg2p [41]. Moreover, these growth defects were alleviated by the expression of TcGFP-AVP1.

To solve the issue of whether ergosterol depletion or abnormal sterols *per se* are the cause of the observed impairment in acidification, we analysed the resistance to Zn^{2+} in other strains devoid of any ergosterol (Fig. 1D). Strains accumulating predominantly fecosterol (*erg2*Δ) showed sensitivity to Zn^{2+} at concentrations close to those observed to inhibit growth in a V-ATPase mutant (*vph1*Δ). However, strains accumulating chiefly ergosta-5,7,24(28)-trienol (*erg4*Δ) or cholesterol (RH 6829) showed reduced sensitivity to Zn^{2+} , and that accumulating principally episterol (*erg3*Δ) displayed no apparent differences compared with a wild-type strain.

3.2 8-dehydrosterols impair H^+-pumping at the vacuole

A possible cause for the observed phenotypes in *erg2Δ* cells could be that 8-dehydrosterols, like other abnormal sterols [42], were affecting protein traffic of the V_0 V-ATPase domain from the endoplasmic reticulum to the Golgi system and thus impairing correct assembly of the V_1 domain on it [43]. We made whole cell extracts from a wild-type W303-1a strain and its *erg2Δ* mutant derivative and analysed the amount of Vph1p associated to Vma1p by co-immunoprecipitation, as marker subunits of V_0 and V_1 domains, respectively (Fig. 2A). However, we did not find any remarkable differences either in the amount of polypeptides precipitated or in the Vph1p/Vma1p ratios between wild-type and *erg2Δ*-derived strains. Still, if ER-to-Golgi system protein transport was affected in any way, this should provoke ER stress and, as a consequence, unfolded protein response (UPR) [44]. To ascertain whether this was the case, we introduced the plasmid pJC104 into W303-1a and *erg2Δ* strains. This 2µ plasmid contains a fusion of four in-tandem copies of a UPR-responsive promoter element driving the expression of the β-galactosidase ORF [45]. Untreated *erg2Δ* cells showed a slightly greater β-galactosidase activity than wild-type cells (less than two-fold) that was not statistically significant (Fig. 2B). Similarly, treatment with tridemorph, an amine fungicide that specifically inhibits Erg2p in yeast [41], did not increase β-galactosidase activity with respect to controls. In contrast, wild-type or *erg2Δ* yeast cells treated with 3 mM DTT,

a known inducer of ER-stress [46], displayed a five- to seven-fold greater β-galactosidase activity, compared with the corresponding untreated cells.

To ascertain if *erg2Δ* phenotypes observed were due to impairment of V-ATPase transport functions, we isolated vacuole vesicles from strains W303-1a and *erg2Δ*. Proton-pumping assays done using these vesicles revealed that vacuole vesicles from *erg2Δ* cells were seriously impaired for H^+ gradient generation (Fig. 2C). In particular, *erg2Δ*-derived vacuolar vesicles displayed a *ca* 2.2-fold smaller rate of proton transport than wild-type ones (163 ± 47 *vs* 359 ± 62 %F min^{-1} mg^{-1} protein ± SE, respectively; n = 3). Similarly, the magnitude of gradient formed was affected to roughly the same extent: under the assay conditions, maximal quenching using wild-type vesicles was 45.4 ± 4.6%, while *erg2Δ*-derived vesicles levelled at 21.3 ± 2.9% (percentage of ACMA fluorescence using 40 µg protein ± SE, n=3). In contrast, the hydrolytic activity of the V-ATPase showed a smaller inhibition, comparing again *erg2Δ* with wild-type: we estimated an activity of 403 ± 26 nmol Pi min^{-1} mg^{-1} protein using wild-type derived vacuolar vesicles *vs* 324 ± 34 nmol Pi min^{-1} mg^{-1} protein using similar preparations obtained from *erg2Δ* cells (averages ± SE, n = 3). *Western* blots using protein markers for the membrane embedded domain V_0 (Vph1p) and the extrinsic V_1 (Vma1p) showed similar levels in both wild-type and *erg2Δ* mutant (Fig. 2D).
We observed that Vph1p was remarkably prone to proteolytic degradation in vacuole preparations from *erg2Δ* mutant cells, suggestive of a conformational change similar to that observed in sterol-deprivation experiments [24]. To analyse this possibility, vacuolar membrane preparations from both wild-type and *erg2Δ* mutants were subjected to trypsin digestion. A time-course analysis (Fig. 2E) confirmed that Vph1p displayed a drop in half-life from 21.7±0.4 min in wild-type cells to 5.4±0.4 min in preparations from *erg2Δ* mutants, in the presence of trypsin.

3.3 Endocytosis phenotypes or erg2Δ cells are alleviated by expression of a H^+-PPase

Some of the most typical phenotypes associated to *ERG2* and V-ATPase deficiency are defects in the endocytic traffic. These defects can be evaluated by the internalization of the lipophilic tracer dye FM4-64. We tested if the expression of TcGFP-AVP1 could alleviate this phenotype (Fig. 3A). Expression of this H^+-pump did not alter significantly the staining pattern in YPC3 wild-type cells, compared with non-transporting soluble PPase (*IPP1*) expressing YPC3; nevertheless, more vacuolar fragmentation could be observed in H^+-PPase expressing cells, a feature already reported in a previous article [39]. As expected, expression of this alternative proton pump restored the ability of *vph1Δ* (SAH6 strain) cells to internalise FM4-64. More importantly, TcGFP-AVP1 also allowed *erg2Δ* (SAH2) cells to internalise this vital dye in a way akin to that observed in wild-type YPC3 cells. Still, this recovery of function was not as complete as that observed in *vph1Δ* cells and the level of plasma membrane residual staining was greater in *erg2Δ* cells than in the latter strain.
A complementary approach was used to confirm that fluid-phase endocytosis was also improved by expression of TcGFP-AVP1. Lucifer Yellow (LY) is a soluble fluorescent vital dye that accumulates in vacuoles only if endocytic traffic is effective. Similar to what was observed in the case of FM4-64, *vph1Δ* yeast cells showed no accumulation of the dye in their vacuoles if *IPP1* was expressed from a plasmid (Fig.3B). However, if vacuolar acidification was restored by means of the H^+-PPase TcRED-AVP1, this mutant showed a notable accumulation of LY. The chimaeric H^+-PPase TcRED-AVP1 was chosen because it provided an efficient and clean complementation of vacuole acidification defects similar to those attained with TcGFP-AVP1 [26] but circumvented the emission of fluorescence in the same range as LY. Yeast cells accumulating 8-dehydrosterols (*erg2Δ*) behaved in the same way as *vph1Δ* cells, namely, they were unable to internalise LY if *IPP1* was expressed episomally, while they showed nearly no differences with a wild-type if TcRED-AVP1 was expressed as an alternative proton pump.

3.4 Mutants in erg2Δ show acidification-dependent exocytosis defects.

Often, links between accumulation of 8-dehydrosterols, like fecosterol, and cell wall defects have been found in both plants and fungi [47, 48]. We measured the sensitivity of *erg2Δ* and *vph1*Δ *mutants* to cell wall damage as the velocity of cell bursting under hypotonic conditions produced by lyticase treatment, a cell wall digesting commercial mixture of enzymes (Fig. 4A). In order to ascertain if acidification defects were involved, we made use of strains dependent on a *GAL1* promotor for the expression of the essential *IPP1* gene. Mutant cells (either *erg2Δ* or *vph1*Δ) expressing ectopically the *IPP1* ORF displayed a markedly increased sensitivity to lyticase compared with their parental strain. However, if these same mutants expressed ectopically the H^+-pumping TcGFP-AVP1, their sensitivity was noticeably reduced in the case of *erg2Δ* and comparable with that observed in a wild-type, in the case of *vph1*Δ.
Cell wall construction depends on materials and enzymes being transported to the outer limit of the cell by exocytosis [49, 50]. We used Pma1p and Suc2p as markers for correct exocytic traffic. Pma1p was found to be mislocalised in part to the vacuolar membrane in the case of the *erg2Δ* mutant, as assessed using fractions enriched in vacuolar vesicles probed with antibodies raised against Pma1p and V-ATPase components (Fig. 4B). However, this mislocallisation could be partially reverted if the H^+-pumping TcGFP-AVP1 was expressed ectopically (Fig. 4C). In contrast, invertase activity (Suc2p) was not affected by mutations in either *ERG2* or *VPH1* genes (Fig. 4D).

3.5 Cells defective in ERG2 accumulate autophagic bodies

Inhibition of V-ATPase activity is widely used to induce autophagy defects. Bearing in mind the previous results, we sought to assess if *erg2Δ* yeast cells were also defective in macroautophagy. To this end, we analysed the accumulation of autophagic bodies under nitrogen starvation conditions, a characteristic phenotype of mutants impaired in the last steps of autophagy, such as vacuolar protease mutants [51]. As expected, cells defective in vacuolar proteases A and B accumulated autophagic bodies if deprived for nitrogen in the growth medium (Fig. 5A) and, consequently, the proportion of cells showing undigested accretions were *ca* 40% of total cells in a culture under these conditions (Fig. 5B). A similar pattern was observed in cells treated with bafilomycin A, a specific V-ATPase inhibitor, or in *vph1Δ* mutants. In the latter cases, the amount of autophagic bodies-displaying cells represented *ca* 50-60% of the culture. Cells defective in *ERG2* also showed a clear phenotype and the percentage of autophagic bodies accumulating cells in a culture reached again *ca* 60%.
We then tested if this phenotype observed in *erg2Δ* cells was also dependent on V-ATPase dysfunction. Strains expressing ectopically the non-transporting pyrophosphatase gene *IPP1* but bearing mutations in either *ERG2*, *STV1* or *VPH1* showed similar defects as those observed earlier, although the extent varied (Fig. 5C); thus SAH2 strains (GAL1prom.-*IPP1 erg2*Δ) showed only *ca* 25% of cells accumulating autophagic bodies, while those derived from W303-1a (see Fig. 5B) exhibited *ca* 60%. Smaller differences were also observed in *stv1Δ and, particularly, in vph1Δ* mutants. Moreover, the presence of an alternative PPi-dependent proton pump (TcGFP-AVP1) increased noticeably the percentage of cells displaying autophagic accretions under normal growth conditions, compared with *IPP1* expressing controls. However, strains expressing a H^+-pumping pyrophosphatase displayed strong reductions in the percentage of cells showing accumulation of autophagic bodies under nitrogen starvation conditions, compared with *IPP1* controls: *ca* 2.8-fold for *erg2*Δ, 3.6-fold for *stv1*Δ and 2.5-fold in the case of *vph1*Δ.

3.6 Yeast erg2Δ cells show no further defects in autophagy

We sought to find out if the macroautophagy phenotype observed in *erg2Δ* mutants conformed to the hypothesis that only the late steps in autophagy were affected due to inhibition of V-ATPase activity. To this end, we analysed the activation of Pho8Δ60p, a truncated form of alkaline

phosphatase that is only active if autophagy is properly induced [35]. As expected, an *atg8Δ* mutant showed a reduced ability to activate Pho8Δ60p (Fig. 6A). Surprisingly, *erg2Δ* and *vph1Δ* mutants showed no differences compared with a wild-type.
Further examination of possible defects in early steps of autophagy and their related vesicular transport pathways were analysed using the processing of the aminopeptidase I (Ape1p) and a GFP-ATG8 fusion protein as markers (Figs 6B and 6C). In contrast to that observed in a *atg4*Δ mutant, Ape1p was correctly transported and processed in both normal conditions (when the cytoplasm-to-vacuole pathway plays a major role in transporting this enzyme to the vacuole for processing) and nitrogen starvation conditions (when the autophagy pathway takes over this function; Fig. 6B) in all strains tested. The only exception was *vph1*Δ strain under nitrogen starvation conditions, when a modest impairment of Ape1p processing was noticeable. Similarly, GFP-Atg8p was observed to accumulate diffusely in the cytosol in all strains tested, while the vacuole displayed a smaller fluorescence intensity (Fig. 6C). Under nitrogen starvation conditions, again, all strains showed greater fluorescence intensity in the vacuoles than in the cytosol, as expected from a correct translocation of GFP-Atg8p to the lumen of this organelle in the process of autophagy.

Autophagy defects translate into lower rates of survival under starvation conditions. In order to assess if *erg2Δ* cells were affected in their ability to survive nitrogen starvation, we measured the capability of these cells to form colonies through time in nitrogen-free minimal medium. To avoid cell death related to inability to synthesise amino acids [52], all strains were transformed with low copy plasmids of the pRS31X series [53] in order to complement any auxotrophy not covered by expression plasmids. Under these conditions, an *atg8Δ* mutant displayed a characteristic low survival rate, compared with wild-type cells: its survival half-time was only 1.7 ± 0.1 days *vs* 14.1 ± 8.6 days for the wild-type SE6210 strain (Fig. 6D; data are average ± S.E., n = 3, in all cases). W303-1a wild-type cells displayed a relatively shorter half-life of only 5.1±0.2 days, compared with the former reference wild-type. Cells devoid of vacuolar ATPase (*vph1Δ*) showed a modest decrease in their survival capability under nitrogen starvation, compared with W303-1a, with an estimated half-time of 3.5±0.2 days. Remarkably, *erg2Δ* cells showed a greater capability to withstand nitrogen starvation than its reference wild-type (W303-1a). Thus, their survival half-time was estimated to be roughly 3-fold greater at 15.0±1.1 days.

3.7 Analysis of vacuolar proteases and lipases in erg2Δ cells

Since accumulation of autophagic bodies are a reflection of an inability to digest autophagocited cargoes, we analysed if defects in either proteases or lipases could be at play. Protease A (PrA, Pep4p) activity was determined as the release of tyrosine from haemoglobin at acidic pH [36] (Fig. 7A). Both *erg2*Δ and *vph1*Δ mutants showed clearly reduced PrA activities (*ca* 61% and 70%, repectively), compared with a wild-type strain; in contrast, *stv1*Δ showed only a modest decrease (*ca* 82%). Nonetheless, the activities observed in all these strains were much greater to those observed in a *pep4*Δ *prb1*Δ strain (*ca* 10% compared with W303-1a).
We also followed the processing and transport of Atg15p, a lipase essential in autophagy [54]. Under nitrogen starvation conditions, a GFP-Atg15p fusion protein was dually localised in the ER and in the vacuole in all strains (Fig. 7B). Furthermore, all strains tested showed glycosylated Atg15p and, upon nitrogen starvation, reduced their protein levels as expected from its transport into the vacuole (data not shown). In addition, we examined if Atg26p, a sterol-glycosyltranferase could be involved. However, under nitrogen starvation conditions, an *atg26*Δ strain did not accumulate autophagic bodies (data not shown).

4. Discussion

In this work, we have shown that 8-dehydrosterols disrupt V-ATPase-dependent organelle

acidification. This explains why mutants bearing a defect on the *ERG2* gene display phenotypic features similar to those found in Vma^- strains. Consequently, expression of an alternative H^+-pump alleviates these phenotypes. It has already been proposed that Δ^{14}-sterols and 14α-methylated sterols exert part of their effects through inhibition of the vacuolar H^+-ATPase in budding yeast and *Candida albicans* [24, 25]. However, the biochemical and cellular consequences of the accumulation of different abnormal sterols may differ significantly; *e. g.*, translocation of proteins from the endoplasmic reticulum (ER) to the Golgi system is inhibited by cholesterol, allocholesterol or dehydrocholesterol but not by lathosterol or cholesta-8(14)-en-3β-ol [42]. Similarly, in *Ustilago maydis*, the proton transport across plasma membrane vesicles was found to be uncoupled by 8-dehydrosterols but no differences were observed in the presence of 14α-methylated sterols [55]. In this respect, our data show that the effects observed in *erg2*Δ mutants or in fungicide-treated cells are actually due to the accumulation of toxic 8-dehydrosterols and not simply by a depletion of ergosterol in their membranes, since other ergosterol-depleted strains show varied degrees of acidification defects ranging from mild to null, compared with a wild-type strain.

In comparison with the effects observed in Δ^{14}-sterols accumulating fungal cells, the present data stand for a somewhat similar mechanism of action for 8-dehydrosterols against the yeast V-ATPase; i.e., they reduce the proton translocation capacity of this pump. Still, Δ^{14}-sterols have been shown to inhibit both ATPase and proton pumping activities to the same extent [25] while 8-dehydrosterols provoke a comparatively smaller effect on V-ATPase hydrolytic activity. A conformational change of the protein or a greater exposure from the lipid bilayer is suggested by a greater sensitivity of subunit a to proteolytic degradation and may be significant in the uncoupling mechanism. The actual reason for this increased sensitivity can only be speculated but two mechanisms spring to mind: on the one hand, 8-dehydrosterols are non-planar molecules that, as such, may have a smaller fatty acid ordering capacity that could lead to a thinner bilayer; this could leave protease-sensitive domains from Vph1p exposed; however, lanosterol is also an 8-dehydrosterol that, although it increases protease sensitivity to yeast V-ATPase subunits [24], it induces no differences in bilayer thickness, as compared with cholesterol or ergosterol [56]. On the other hand, V-ATPase V_0 domain subunits may require direct contact with sterols for stability and H^+-transport and the interaction with 8-unsaturated sterols may provoke disfunctions. This is in agreement with the association of V-ATPases with lipid rafts in mammalian cells [57, 58] and with the requirement for cholesterol that the chromaffin granule V-ATPase has for proton pumping but not for ATP hydrolysis in reconstituted vesicles [59].

In our hands, inhibition of the proton pumping activity of the V-ATPase by 8-dehydrosterols had clear effects on endo- and exocytosis (Pma1p pathway) but did not prevent membrane fusion-dependent translocation of cargoes to the plasma membrane through the Suc2p pathway or to the vacuole through the CVT, ER/Golgi-to-vacuole or autophagy pathways, as assessed by invertase and Pho8Δ60p assays, localisation and assembly of V-ATPase and fluorescence microscopy localisation of GFP-Atg15p and GFP-Atg8p. Although paradoxical this is not extraordinary: dependence on V-ATPase for lumen acidification may differ between pathways and each organelle typically displays a different characteristic pH gradient with respect to the cytosol. Conversely, inhibition of the V-ATPase is unlikely to be complete *in vivo.* Furthermore, there exist some ATPase-independent luminal acidification processes [60] that could suffice to provide the small pH gradients necessary [2].

Endocytosis is a remarkable example of the effects of 8-dehydrosterols on cellular functions with an unresolved mechanism to date [23]. Notably, this process seems to be especially dependent on luminal acidification, since both *erg2Δ* and *vph1Δ* cells show distinctly reduced intakes of LY and FM4-64. Consequently, endocytosis defects in in these mutants were relieved by the introduction of an alternative proton pump, providing a direct causative link between abnormal sterols, V-ATPase activity and a process at the cellular level. Also, the present data show for the first time that cells

defective in sterol-Δ^8,Δ^7-isomerase activity exhibit a V-ATPase-dependent exocytosis defect affecting the Pma1p pathway since, like *vph1*Δ mutants, they partially mislocalise this protein to the vacuolar membrane [61] and the expression of an alternative H^+-pump reverses this defect. Moreover, this may be at the root of the cell wall defects observed in this and other studies [48] since cell wall synthesising and remodelling enzymes are transported to the plasma membrane following the exocytic routes, often the same one as Pma1p [49, 62].

Bafilomycin A is routinely used in mammalian systems as a specific V-ATPase inhibitor useful to dissect autophagy-dependent processes. Although there is some debate on the mechanisms, it is considered that inhibition of V-ATPase can block the autophagic flux in mammals [63]. Likewise, yeast V-ATPase mutants are accredited autophagy mutants because lack of V-ATPase activity blocks the maturation of proteases and other hydrolases necessary for breaking down internalised cargoes [64]. This, together with our previous results on membrane traffic, led us to hypothesise that cells defective in V-ATPase activity, such as 8-dehydrosterol accumulating cells, would display autophagic deficiencies. In this sense, it was puzzling to a certain extent to find that *erg2*Δ and Vma^- mutants *vph1*Δ and *stv1*Δ showed no impairment in autophagic flux. As mentioned before, a plausible explanation is that the small gradient necessary for membrane fusion [2] may be achieved through V-ATPase–independent mechanisms [60]. On the other hand, autophagic bodies were found to accumulate, although this was not accompanied by a loss of survival capacity under nitrogen starvation conditions. To the authors' knowledge, it has not been evaluated to date to which extent it is necessary to impair protease activity to observe accumulation of autophagic bodies; on the contrary, studies this far usually made use of protease deletion mutants or high inhibitor concentrations. In this respect, our data point out that impairment of vacuo/lysosomal acidification has mild but effective consequences on protease A/Pep4p activity. This is consistent with mutants affected in V-ATPase proton pumping, such as *stv1*Δ, *vph1*Δ, and *erg2*Δ mutants, not inducing the full range of phenotypes observed in other autophagy mutants; particularly, reduced survival under nitrogen starvation conditions, ineffective aminopeptidase I processing or reduced activity in the modified alkaline phosphatase Pho8Δ60p assay. The latter two proteins rely on proteolysis by Prb1p for activation [65], an event occurring in the vacuolar lumen. Prb1p itself undergoes a series of proteolytic modifications *en route* to the vacuole, being finally processed in the lumen by Pep4p in a luminal low pH dependent manner [64]. Hence, we posit a model where 8-dehydrosterols inhibit lumen acidification which, in turn, results in a modest reduction in protease A activity that drive autophagic body accumulation on nitrogen starvation conditions; nevertheless, this chain of events is insufficient to hamper autophagy severely or affect processing of vacuolar resident proteins. This may have implications on the interpretation of experiments where bafilomycin A is used to probe autophagy.

In algae, many protists and higher plants, V-ATPases and H^+-PPases share a common location at the vacuolar membrane. Recently, we have shown that the latter type of pumps is sufficient for acidifying internal compartments in yeast [26]. When grown on glucose, YPC3 yeast cells expressing TcGFP-AVP1 reflect closely the situation found in plant cells in terms of PPi homeostasis and proton transport across the tonoplast. These yeast cells have been shown to display a vigorous endocytosis, nearly correct exocytic transport of Pma1p, and a robust cell wall while accumulating abnormal sterols. Thus, the presence of a double set of H^+ pumps may explain why algae and plants can tolerate sterol biosynthesis inhibitors used as crop protecting fungicides, even though they do affect the sterol composition of their cell membranes [66].

Mutations in *ERG2* and, consequently, the accumulation of 8-dehydrosterols, is not lethal in yeast but in more complex organisms like humans (e.g. males affected by CDPX2) usually the embryonic development cannot be completed [67]. The current line of thought is inclined towards abnormal sterols altering Hedgehog signalling. Nevertheless, the present data, without casting off the former hypothesis, introduces a novel player and possible mechanism, namely V-ATPase inhibition. Work

is needed to ascertain if V-ATPase defects phenocopy CDPX2 and if cells from CDPX2-affected individuals or models show diminished V-ATPase activities in tissues such as cartilage.

In this report, we also demonstrate the suitability of a plant vacuolar H^+-pumping PPase to discern proton gradient-dependent and independent cellular events in yeast. Moreover, it extends this value beyond that reported recently for the study of yeast V-ATPase physical involvement in homotypic vacuole fusion using a similar approach [2].

All in all, the present study shows that 8-dehydrosterols provoke an inability to acidify yeast vacuoles and possibly other vesicular organelles. This, on its turn, is at the root of the defects on endocytosis, exocytosis, cell wall maintenance and autophagy observed in these mutants. The presence of a double set of primary H^+ pumps in 8-dehydrosterol-accumulating cells alleviates phenotypes and allows cells to proliferate under restrictive conditions. As stated above, the implications of these results span multiple aspects in eukaryotic cell biology that range from genetic rare diseases in humans to fungicide tolerance in plants and certain fungi.

5. Acknowledgements

The authors wish to thank Drs J. Rine and A. Mayer for their kind gifts of strains used in this study or in preliminary experiments. Also thanks to Drs D.T. Cooke and D.T. Clarkson for initial inputs on this field and Ms I. Jiménez for her invaluable technical assistance. This work was funded by the Andalusian Regional Government and the Spanish Ministry of Science and Innovation through their support to PAIDI group BIO-261 and grant BFU2010-15622, all of them partially funded by the EU FEDER program. PAIDI group BIO-261 belongs to the CeiA3 and AndaluciaTECH University Campuses of International Excellence.
The authors declare not to have any conflict of interests regarding this publication.

6. References

[1] T.L. Baars, S. Petri, C. Peters, A. Mayer, Role of the V-ATPase in regulation of the vacuolar fission-fusion equilibrium, Mol Biol Cell, 18 (2007) 3873-3882.
[2] E.M. Coonrod, L.A. Graham, L.N. Carpp, T.M. Carr, L. Stirrat, K. Bowers, N.J. Bryant, T.H. Stevens, Homotypic vacuole fusion in yeast requires organelle acidification and not the V-ATPase membrane domain, Dev. Cell, 27 (2013) 462-468.
[3] C. Huang, A. Chang, pH-dependent cargo sorting from the Golgi, J Biol Chem, 286 (2011) 10058-10065.
[4] D. Ramirez-Montealegre, D.A. Pearce, Defective lysosomal arginine transport in juvenile Batten disease, Hum Mol Genet, 14 (2005) 3759-3773.
[5] D. Mijaljica, M. Prescott, R.J. Devenish, V-ATPase engagement in autophagic processes, Autophagy, 7 (2011) 666-668.
[6] V. Pasapula, G. Shen, S. Kuppu, J. Paez-Valencia, M. Mendoza, P. Hou, J. Chen, X. Qiu, L. Zhu, X. Zhang, D. Auld, E. Blumwald, H. Zhang, R. Gaxiola, P. Payton, Expression of an *Arabidopsis* vacuolar H^+-pyrophosphatase gene (AVP1) in cotton improves drought- and salt tolerance and increases fibre yield in the field conditions, Plant Biotechnol J, 9 (2011) 88-99.
[7] J. Zhang, J. Li, X. Wang, J. Chen, OVP1, a vacuolar H^+-translocating inorganic pyrophosphatase (V-PPase), overexpression improved rice cold tolerance, Plant Physiol Biochem, 49 (2011) 33-38.
[8] A. Hernandez, G. Serrano-Bueno, J.R. Perez-Castineira, A. Serrano, Intracellular proton pumps as targets in chemotherapy: V-ATPases and cancer, Curr Pharm Des, 18 (2012) 1383-1394.
[9] Y.M. Drozdowicz, P.A. Rea, Vacuolar H(+) pyrophosphatases: from the evolutionary backwaters into the mainstream, Trends Plant Sci, 6 (2001) 206-211.

[10] M. Maeshima, Tonoplast Transporters: Organization and Function, Annu Rev Plant Physiol Plant Mol Biol, 52 (2001) 469-497.
[11] J.R. Pérez-Castiñeira, R. Gómez-García, R.L. López-Marqués, M. Losada, A. Serrano, Enzymatic systems of inorganic pyrophosphate bioenergetics in photosynthetic and heterotrophic protists: remnants or metabolic cornerstones?, Int Microbiol, 4 (2001) 135-142.
[12] R.I. Kelley, G.E. Herman, Inborn errors of sterol biosynthesis, Annu Rev Genomics Hum Genet, 2 (2001) 299-341.
[13] N. Braverman, P. Lin, F.F. Moebius, C. Obie, A. Moser, H. Glossmann, W.R. Wilcox, D.L. Rimoin, M. Smith, L. Kratz, R.I. Kelley, D. Valle, Mutations in the gene encoding 3 β-hydroxysteroid-Δ^8, Δ^7-isomerase cause X-linked dominant Conradi-Hunermann syndrome, Nat Genet, 22 (1999) 291-294.
[14] A. Rahier, P. Schmitt, B. Huss, P. Benveniste, E.H. Pommer, Chemical structure-activity relationships of the inhibition of sterol biosynthesis by N-substituted morpholines in higher plants, Pestic Biochem Physiology, 25 (1986) 112-124.
[15] H. Buchenauer, E. Röhner, Effect of triadimefon and triadimenol on growth of various plant species as well as on gibberellin content and sterol metabolism in shoots of barley seedlings, Pestic Biochem Physiology, 15 (1981) 58-70.
[16] W. Köller, Isomers of sterol synthesis inhibitors: Fungicidal effects and plant growth regulator activities, Pestic Sci, 18 (1987) 129-147.
[17] A.-N. Petit, F. Fontaine, P. Vatsa, C. Clément, N. Vaillant-Gaveau, Fungicide impacts on photosynthesis in crop plants, Photosyn. Res., 111 (2012) 315-326.
[18] M. Souter, J. Topping, M. Pullen, J. Friml, K. Palme, R. Hackett, D. Grierson, K. Lindsey, hydra Mutants of *Arabidopsis* are defective in sterol profiles and auxin and ethylene signaling, Plant Cell, 14 (2002) 1017-1031.
[19] M. Bard, R.A. Woods, D.H. Barton, J.E. Corrie, D.A. Widdowson, Sterol mutants of *Saccharomyces cerevisiae*: chromatographic analyses, Lipids, 12 (1977) 645-654.
[20] P.M. Kane, The where, when, and how of organelle acidification by the yeast vacuolar H^+-ATPase, Microbiol Mol Biol Rev, 70 (2006) 177-191.
[21] M.A. Pagani, A. Casamayor, R. Serrano, S. Atrian, J. Ariño, Disruption of iron homeostasis in *Saccharomyces cerevisiae* by high zinc levels: a genome-wide study, Mol Microbiol, 65 (2007) 521-537.
[22] R. Serrano, D. Bernal, E. Simon, J. Ariño, Copper and Iron Are the Limiting Factors for Growth of the Yeast *Saccharomyces cerevisiae* in an Alkaline Environment, J Biol Chem, 279 (2004) 19698-19704.
[23] A.L. Munn, A. Heese-Peck, B.J. Stevenson, H. Pichler, H. Riezman, Specific sterols required for the internalization step of endocytosis in yeast, Mol Biol Cell, 10 (1999) 3943-3957.
[24] Y. Zhang, R. Rao, Beyond ergosterol: Linking pH to antifungal mechanisms, Virulence, 1 (2010) 551-554.
[25] Y.-Q. Zhang, S. Gamarra, G. Garcia-Effron, S. Park, D.S. Perlin, R. Rao, Requirement for ergosterol in V-ATPase function underlies antifungal activity of azole drugs, PLoS pathogens, 6 (2010) e1000939.
[26] J.R. Perez-Castiñeira, A. Hernandez, R. Drake, A. Serrano, A plant proton-pumping inorganic pyrophosphatase functionally complements the vacuolar ATPase transport activity and confers bafilomycin resistance in yeast, Biochem J, 437 (2011) 269-278.
[27] R.D. Gietz, R.A. Woods, Transformation of yeast by lithium acetate/single-stranded carrier DNA/polyethylene glycol method, Methods Enzymol, 350 (2002) 87-96.
[28] F. Sherman, Getting started with yeast, Methods Enzymol, 194 (1991) 3-21.
[29] A. Hernandez, X. Jiang, B. Cubero, P.M. Nieto, R.A. Bressan, P.M. Hasegawa, J.M. Pardo, Mutants of the *Arabidopsis thaliana* cation/H^+ antiporter AtNHX1 conferring increased salt tolerance in yeast: the endosome/prevacuolar compartment is a target for salt toxicity, J Biol Chem, 284 (2009) 14276-14285.
[30] A. Hernandez, D.T. Cooke, D.T. Clarkson, Lipid composition and proton transport in

Penicillium cyclopium and *Ustilago maydis* plasma membrane vesicles isolated by two-phase partitioning, Biochim Biophys Acta, 1195 (1994) 103-109.
[31] N. Perzov, V. Padler-Karavani, H. Nelson, N. Nelson, Characterization of yeast V-ATPase mutants lacking Vph1p or Stv1p and the effect on endocytosis, J Exp Biol, 205 (2002) 1209-1219.
[32] A. Wiederkehr, K.D. Meier, H. Riezman, Identification and characterization of *Saccharomyces cerevisiae* mutants defective in fluid-phase endocytosis, Yeast, 18 (2001) 759-773.
[33] S. Raths, J. Rohrer, F. Crausaz, H. Riezman, end3 and end4: two mutants defective in receptor-mediated and fluid-phase endocytosis in *Saccharomyces cerevisiae*, J Cell Biol, 120 (1993) 55-65.
[34] A. Goldstein, J.O. Lampen, Beta-D-fructofuranoside fructohydrolase from yeast, Methods Enzymol, 42 (1975) 504-511.
[35] T. Noda, D.J. Klionsky, The quantitative Pho8Delta60 assay of nonspecific autophagy, Methods Enzymol, 451 (2008) 33-42.
[36] E.W. Jones, Vacuolar proteases in yeast *Saccharomyces cerevisiae*, Methods Enzymol, 185 (1990) 372-386.
[37] J. Sambrook, E.F. Fritsch, T. Maniatis, Molecular Cloning: A Laboratory Manual, 2nd. ed. ed., Cold Spring Harbor Laboratory Press, Place Published, 1989.
[38] C.L. Ladner, J. Yang, R.J. Turner, R.A. Edwards, Visible fluorescent detection of proteins in polyacrylamide gels without staining, Anal Biochem, 326 (2004) 13-20.
[39] R. Drake, A. Serrano, J.R. Perez-Castiñeira, N-terminal chimaeras with signal sequences enhance the functional expression and alter the subcellular localization of heterologous membrane-bound inorganic pyrophosphatases in yeast, Biochem J, 426 (2010) 147-157.
[40] L.M. Ramsay, G.M. Gadd, Mutants of *Saccharomyces cerevisiae* defective in vacuolar function confirm a role for the vacuole in toxic metal ion detoxification, FEMS Microbiol Lett, 152 (1997) 293-298.
[41] R.I. Baloch, E.I. Mercer, Inhibition of sterol Δ^8, Δ^7-isomerase and Δ^{14}-reductase by fenpropimorph, tridemorph and fenpropidin in cell-free enzyme systems from *Saccharomyces cerevisiae*, Phytochemistry, 26 (1987) 663-668.
[42] I. Nilsson, H. Ohvo-Rekila, J.P. Slotte, A.E. Johnson, G. von Heijne, Inhibition of protein translocation across the endoplasmic reticulum membrane by sterols, J Biol Chem, 276 (2001) 41748-41754.
[43] M. Forgac, Vacuolar ATPases: rotary proton pumps in physiology and pathophysiology, Nat Rev Mol Cell Biol, 8 (2007) 917-929.
[44] K. Kohno, How Transmembrane Proteins Sense Endoplasmic Reticulum Stress, Antioxid Redox Signal, 9 (2007) 2295-2303.
[45] J.S. Cox, P. Walter, A novel mechanism for regulating activity of a transcription factor that controls the unfolded protein response, Cell, 87 (1996) 391-404.
[46] E. Jämsä, M. Simonen, M. Makarow, Selective retention of secretory proteins in the yeast endoplasmic reticulum by treatment of cells with a reducing agent, Yeast 10 (1994) 355-370.
[47] V. Meyer, R.A. Damveld, M. Arentshorts, U. Stahl, C.A.M.J. J., A.F.J. Ram, Survival in the Presence of Antifungals, Journal of Biological Chemistry, 282 (2007) 32935-32948.
[48] K. Schrick, S. Fujioka, S. Takatsuto, Y.-d. Stierhof, H. Stransky, S. Yoshida, G. Jurgens, A link between sterol biosynthesis, the cell wall, and cellulose in *Arabidopsis*, The Plant Journal, 38 (2004) 227-243.
[49] E. Harsay, A. Bretscher, Parallel secretory pathways to the cell surface in yeast, J Cell Biol, 131 (1995) 297-310.
[50] C. Kurischko, V.K. Kuravi, N. Wannissorn, P.A. Nazarov, M. Husain, C. Zhang, K.M. Shokat, J.M. McCaffery, F.C. Luca, The yeast LATS/Ndr kinase Cbk1 regulates growth via Golgi-dependent glycosylation and secretion, Mol Biol Cell, 19 (2008) 5559-5578.
[51] K. Takeshige, M. Baba, S. Tsuboi, T. Noda, Y. Ohsumi, Autophagy in yeast demonstrated with proteinase-deficient mutants and conditions for its induction, J Cell Biol, 119 (1992) 301-311.
[52] V.M. Boer, S. Amini, D. Botstein, Influence of genotype and nutrition on survival and metabolism of starving yeast, Proc Natl Acad Sci U S A, 105 (2008) 6930-6935.

[53] R.S. Sikorski, P. Hieter, A system of shuttle vectors and yeast host strains designed for efficient manipulation of DNA in *Saccharomyces cerevisiae*, Genetics, 122 (1989) 19-27.
[54] U.D. Epple, I. Suriapranata, E.L. Eskelinen, M. Thumm, Aut5/Cvt17p, a putative lipase essential for disintegration of autophagic bodies inside the vacuole, J Bacteriol, 183 (2001) 5942-5955.
[55] A. Hernandez, D.T. Cooke, D.T. Clarkson, Effects of Abnormal-Sterol Accumulation on *Ustilago maydis* Plasma Membrane H^+ -ATPase Stoichiometry and Polypeptide Pattern, J Bacteriol, 180 (1998) 412-415.
[56] J. Pencer, M.P. Nieh, T.A. Harroun, S. Krueger, C. Adams, J. Katsaras, Bilayer thickness and thermal response of dimyristoylphosphatidylcholine unilamellar vesicles containing cholesterol, ergosterol and lanosterol: a small-angle neutron scattering study, Biochim Biophys Acta, 1720 (2005) 84-91.
[57] C. Lafourcade, K. Sobo, S. Kieffer-Jaquinod, J. Garin, F. Gisou, Regulation of the V-ATPase along the endocytic pathway occurs through reversible subunit association and membrane localization, PLoS ONE, 3 (2008) e2758-e2758.
[58] K. Yoshinaka, H. Kumanogoh, S. Nakamura, S. Maekawa, Identification of V-ATPase as a major component in the raft fraction prepared from the synaptic plasma membrane and the synaptic vesicle of rat brain, Neurosci Lett, 363 (2004) 168-172.
[59] J.R. Perez-Castiñeira, D.K. Apps, Vacuolar H(+)-ATPase of adrenal secretory granules. Rapid partial purification and reconstitution into proteoliposomes, Biochem J, 271 (1990) 127-131.
[60] P.J. Plant, M.F. Manolson, S. Grinstein, N. Demaurex, Alternative mechanisms of vacuolar acidification in H(+)-ATPase-deficient yeast, J Biol Chem, 274 (1999) 37270-37279.
[61] N. Perzov, H. Nelson, N. Nelson, Altered distribution of the yeast plasma membrane H^+-ATPase as a feature of vacuolar H^+-ATPase null mutants, J Biol Chem, 275 (2000) 40088-40095.
[62] D.H. Roh, B. Bowers, H. Riezman, E. Cabib, Rho1p mutations specific for regulation of beta(1-->3)glucan synthesis and the order of assembly of the yeast cell wall, Mol Microbiol, 44 (2002) 1167-1183.
[63] D.J. Klionsky, Z. Elazar, P.O. Seglen, D.C. Rubinsztein, Does bafilomycin A1 block the fusion of autophagosomes with lysosomes?, Autophagy, 4 (2008) 849-950.
[64] C.L. Parr, R.A. Keates, B.C. Bryksa, M. Ogawa, R.Y. Yada, The structure and function of *Saccharomyces cerevisiae* proteinase A, Yeast, 24 (2007) 467-480.
[65] K.A. Hecht, A.F. O'Donnell, J.L. Brodsky, The proteolytic landscape of the yeast vacuole, Cell Logist, 4 (2014) e28023.
[66] J.-x. He, S. Fujioka, T.-c. Li, S.G. Kang, H. Seto, S. Takatsuto, S. Yoshida, J.-c. Jang, Sterols Regulate Development and Gene Expression in *Arabidopsis*, Plant Physiol, 131 (2003) 1258-1269.
[67] J. Canueto, M. Giros, R. Gonzalez-Sarmiento, The role of the abnormalities in the distal pathway of cholesterol biosynthesis in the Conradi-Hunermann-Happle syndrome, Biochim Biophys Acta, (2013).
[68] B.S.J. Davies, H.S. Wang, J. Rine, Dual Activators of the Sterol Biosynthetic Pathway of *Saccharomyces cerevisiae*: Similar Activation/Regulatory Domains but Different Response Mechanisms, Mol Cell Biol, 25 (2005) 7375-7385.
[69] C.M. Souza, T.M.E. Schwabe, H. Pichler, B. Ploier, E. Leitner, X.L. Guan, M.R. Wenk, I. Riezman, H. Riezman, A stable yeast strain efficiently producing cholesterol instead of ergosterol is functional for tryptophan uptake, but not weak organic acid resistance, Metabolic Engineering, 13 (2011) 555-569.
[70] J.S. Robinson, D.J. Klionsky, L.M. Banta, S.D. Emr, Protein sorting in *Saccharomyces cerevisiae*: isolation of mutants defective in the delivery and processing of multiple vacuolar hydrolases, Mol Cell Biol, 8 (1988) 4936-4948.
[71] J. Kim, W.P. Huang, D.J. Klionsky, Membrane recruitment of Aut7p in the autophagy and cytoplasm to vacuole targeting pathways requires Aut1p, Aut2p, and the autophagy conjugation complex, J Cell Biol, 152 (2001) 51-64.
[72] M.E. Perez-Perez, M. Zaffagnini, C.H. Marchand, J.L. Crespo, S.D. Lemaire, The yeast

autophagy protease Atg4 is regulated by thioredoxin, Autophagy, 10 (2014) 1953-1964.
[73] R. Dawaliby, A. Mayer, Microautophagy of the nucleus coincides with a vacuolar diffusion barrier at nuclear-vacuolar junctions, Mol Biol Cell, 21 (2010) 4173-4183.

FIGURE LEGENDS

Figure 1.
Complementation of vacuole phenotypes by heterologous expression of a plant H^+-pumping PPase in *stv1Δ*, *vph1Δ* and *erg2Δ* yeast mutants. Except where indicated, all strains are derivatives of YPC3 (*IPP1* under GAL1 promoter). (A) A GFP-chimaera of AVP1 (TcGFP-AVP1), the K^+-dependent H^+-pumping PPase from *Arabidopsis thaliana*, complements phenotypic growth defects in *vph1Δ* mutants. Yeast cultures were grown as described in Materials and Methods to early stationary phase. From left to right, spots correspond to *ca* 10^4, 10^3, 10^2 and 10 cells seeded onto the corresponding plate, respectively. Spots in top and bottom pictures correspond to the same plate, where irrelevant spots had been eliminated for clarity. (B) TcGFP-AVP1 complements phenotypic growth defects in an *erg2Δ* background. Spots as in panel A. (C) Tridemorph, an Erg2p inhibitor, induces V-ATPase defects. Strain used is YPC3 (*IPP1* under GAL1 promoter) transformed with the indicated plasmids. YPD plates were supplemented with 1.5 μM tridemorph and 2 mM $ZnSO_4$, where indicated. Spots as in A. (D) V-ATPase defects are dependent on the sterol species present in membranes, not on depletion of ergosterol. Mutants in *ERG* genes are derivatives of W303-1a; RH 6829 (a cholesterol only-engineered strain) is a derivative of RH 6822. YPD plates were supplemented with $ZnSO_4$, where and as indicated. Amounts of cells inoculated per spot as in A. All media are complex YP media supplemented with the indicated carbon sources and under the indicated conditions.

Figure 2.
8-dehydrosterols impair V-ATPase proton pumping activity. (A) Quantification of global V-ATPase assembly. Detergent-solubilised whole cell extracts were subjected to immunoprecipitation (IP) with a monoclonal antibody against Vma1p and analysed by *Western* blotting using anti-Vma1p and anti-Vph1p antibodies. One hundred micrograms of whole cell protein preparation were used per IP. For comparison, inputs represent 20% of the total protein used in the co-IP assay. Mock: IP in the absence of cell extract. Strains: W303-1a and JRY7773 (*erg2Δ*) (B) Evaluation of 8-dehydrosterol-induced ER stress. Yeast cells were grown to early-log phase and treated, as indicated, for 5 h prior analysis. Activity associated to ER-stress was measured as the induction of expression of β-galactosidase driven from UPR promoter elements (4 x UPRE, pJC104). Activity of β-galactosidase, in Miller units, was referred to that found in untreated W303-1a. Solid bars: untreated strain, open bars: 3 μM tridemorph treatment, hashed bars: 3mM dithiothreitol treatment. Strains: W303-1a and JRY7773 (*erg2Δ*). (C) Representative traces of proton pumping assays using ACMA and vacuolar membrane preparations from *erg2Δ* and W303-1a cells. Forty micrograms of membrane preparation were used per assay. Arrows indicate the timing of corresponding additions. (D) Levels of Vph1p and Vma1p in vacuole membrane vesicles as assayed by *Western* blotting. Four micrograms of protein were applied per lane. Loading was estimated by in-gel TETF and referred to values observed on the W303-1a lane. Strains as in panel A. (E) Trypsin susceptibility assay. Five microgram aliquots of vacuole vesicle protein were taken at the indicated times and Vph1p levels analysed by *Western* blot. A typical experiment is presented on the left panel. Protein quantitation of three independent experiments (mean AU±SE) is shown on the right panel. Open circles: *erg2Δ* mutant-derived vacuolar vesicles; solid circles: vacuolar membranes obtained from the wild-type control. Strains used as in panel A.

Figure 3.
An alternative H^+-pump alleviates endocytosis defects in *erg2Δ* and *vph1Δ* mutants. All strains are derivatives of YPC3. (A) Endocytosis of the fluorescent vital dye FM4-64. Yeast strains were grown to mid-log phase and later pulse-labelled with FM4-64 for 30 min on ice, washed and chased for 60 additional min to display intracellular compartments. Nomarsky, Nomarsky differential interference contrast; FM4-64, fluorescence of FM4-64. Strains are derivatives of W303-1a. (B) Endocytosis of the soluble fluorescent vital dye Lucifer Yellow. Yeast strains were grown to mid-log phase and later

stained with Lucifer Yellow to reveal fluid-phase endocytosis. Top panel, microscopic evaluation of endocytosis. Nomarsky: Nomarsky differential interference contrast; LY: fluorescence from Lucifer Yellow. Lower panel, quantitation of LY uptake as the percentage of cells showing fluorescent vacuoles. Open bars, cells expressing ectopically *IPP1*; closed bars, cells expressing TcRED-AVP1 ectopically. All strains are derivatives of YPC3 (genomic *IPP1* under GAL1 promotor) grown on glucose.

Figure 4.
Acidification-dependent defects in cell wall and exocytosis. (A) Cell wall resistance to degrading enzymes (lyticase) assessed as the velocity of cell bursting in hypotonic medium. Open bars, cells expressing ectopically *IPP1*; closed bars, cells expressing TcGFP-AVP1 ectopically. All strains are derivatives of YPC3 (genomic *IPP1* under GAL1 promotor) grown on glucose. (B) Mislocalisation of Pma1p to the vacuole. Vacuole vesicle (4 µg) and whole cell (20 µg) extracts were probed with antibodies raised against the indicated polypeptides. Loading was estimated by in-gel TETF and referred to values observed on the corresponding W303-1a lane. (C) Alleviation of Pma1p mislocalisation. Vacuole vesicle extracts (4 µg) were probed with antibodies raised against the indicated polypeptides. Where indicated, YPC3-derived strains were used (*GAL1p::IPP1*); pIPP1 and pTcGFP-AVP1 denote strains transformed with expression plasmids bearing the indicated constructs. Loading was estimated by in-gel TETF and referred to values observed on the W303-1a lane. (D) Estimation of exocytosis through the Suc2p-pathway. Cells were grown on 5% YPD to Abs600≈0.8 and invertase secretion induced by resuspension in 0.1% glucose YPD. At indicated times, aliquots were taken to determine periplasmic and total invertase activity. *Sec18*^{ts} strain was grown at 23 ^{o}C until 10 min prior to induction of exocytosis, when it was placed at 37 ^{o}C for the duration of the experiment. All strains are derivatives of W303-1a, except *Sec18*^{ts} (derivative of RH1800).

Figure 5.
Accumulation of autophagic bodies. (A) Autophagic bodies as observed by Nomarsky optics in the indicated strains and treatments under normal and nitrogen starvation growth conditions for 5 h. Strains used are derivatives of W303-1a except *pep4*Δ *prb1*Δ (BJ3505). Arrows denote autophagic bodies (B) Quantification of the proportion of cells displaying accumulation of autophagic bodies under normal growth and nitrogen starvation conditions for 5 h. Same strains as in panel A. Open bars: normal growth conditions; solid bars: nitrogen starvation conditions. (C) Proportion of cells expressing *IPP1* or *TcGFP-AVP1* displaying autophagic bodies under normal and nitrogen starvation conditions for 5 h. Strains used were derivatives of YPC3. Normal growth medium: solid black and white bars; nitrogen starvation conditions: hatched and grey bars; black and hatched bars depict IPP1 expressing cells; white and solid grey bars represent TcGFP-AVP1 expressing strains. For both B and C panels, a minimum of 300 cells were counted per experiment. Data are means ± SE of three independent experiments.

Figure 6.
Autophagy defects in *erg2Δ* mutants do not imply impairment of cargo translocation to the vacuole. (A) Alkaline phosphatase assays from *pho8Δ60* cells. Bulk delivery and accomplishment of autophagy was assessed as alkaline phosphatase activity using α-naphtol as substrate in cells expressing a truncated form of the vacuolar inducible alkaline phosphatase under normal growth and nitrogen starvation conditions for 3 h. F.U.: fluorescence units. Open bars: normal growth conditions; solid bars: nitrogen starvation conditions. Data are means ± SE of three independent experiments. All strains were derivatives of SAH27 (see Table 1). (B) Transport and processing of aminopeptidase I under normal and nitrogen starvation conditions. Whole cell extracts (50 µg) were probed with an anti-Ape1p antibody. All strains are derivatives of W303-1a, except *atg4*Δ (SEY6210). Loading was estimated by in-gel TETF and referred to values observed on the *atg4*Δ

control lane. (C) Localisation of a GFP-Atg8p chimaera in cells subjected to normal growth or nitrogen starvation conditions for 3 h. Nomarsky: Nomarsky differential interference contrast; GFP: Green fluorescent protein. All strains are derivatives of W303-1a (D) Cell survival under nitrogen starvation. Stationary phase-cells were kept in nitrogen source-free minimal medium and the viability was probed at the indicated times as the capacity of individual cells to form colonies (CFU, colony forming units) and expressed as a percentage of total cells in the culture. Open squares: wild-type (SEY6210); closed squares, *atg8Δ* (WPHYD7); open circles: wild-type (W303-1a); closed circles: *erg2Δ* (SAH2); open triangles: *vph1Δ* (SAH7).

Figure 7.
Analysis of vacuolar protease and lipase defects in V-ATPase and *erg2*Δ mutants. (A) Protease A activity. Cells were grown to stationary phase and protease activity assayed using whole cell extracts as the liberation of tyrosine from haemoglobin at pH 3.2. All strains are W303-1a derivatives, except *pep4*Δ *prb1*Δ (BJ3505). (B) Localisation of the Atg15p lipase in the vacuole under nitrogen starvation conditions (3h). All strains are derivatives of W303-1a where the genomic copy of the ATG15 ORF has been modified to include an in-frame GFP tag at the *N*-terminus of the translated protein. Nomarsky: Nomarsky differential interference contrast; GFP: Green fluorescent protein.

Figure 1
(Fitting 1.5 columns)

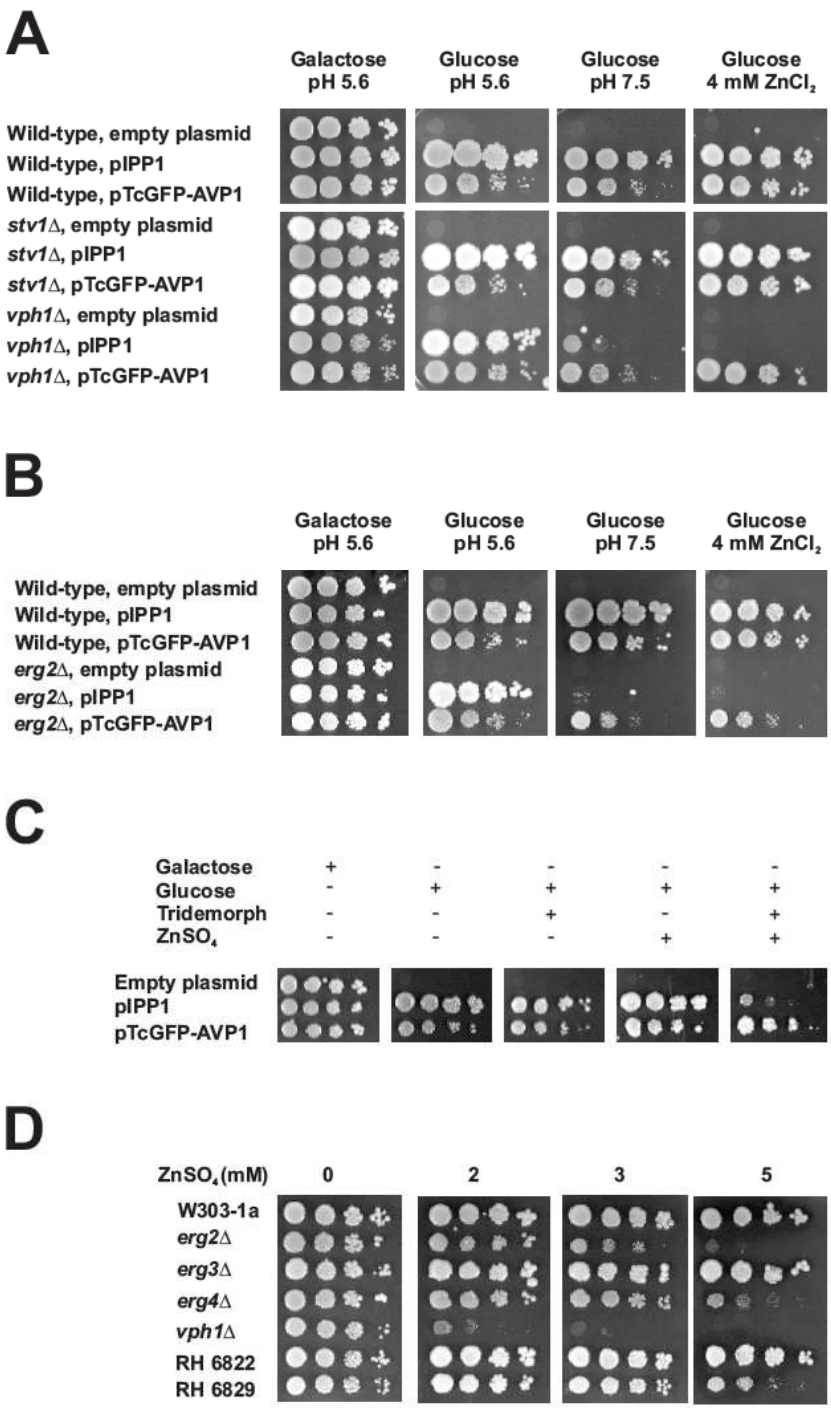

Figure 2
(Fitting 2-column)

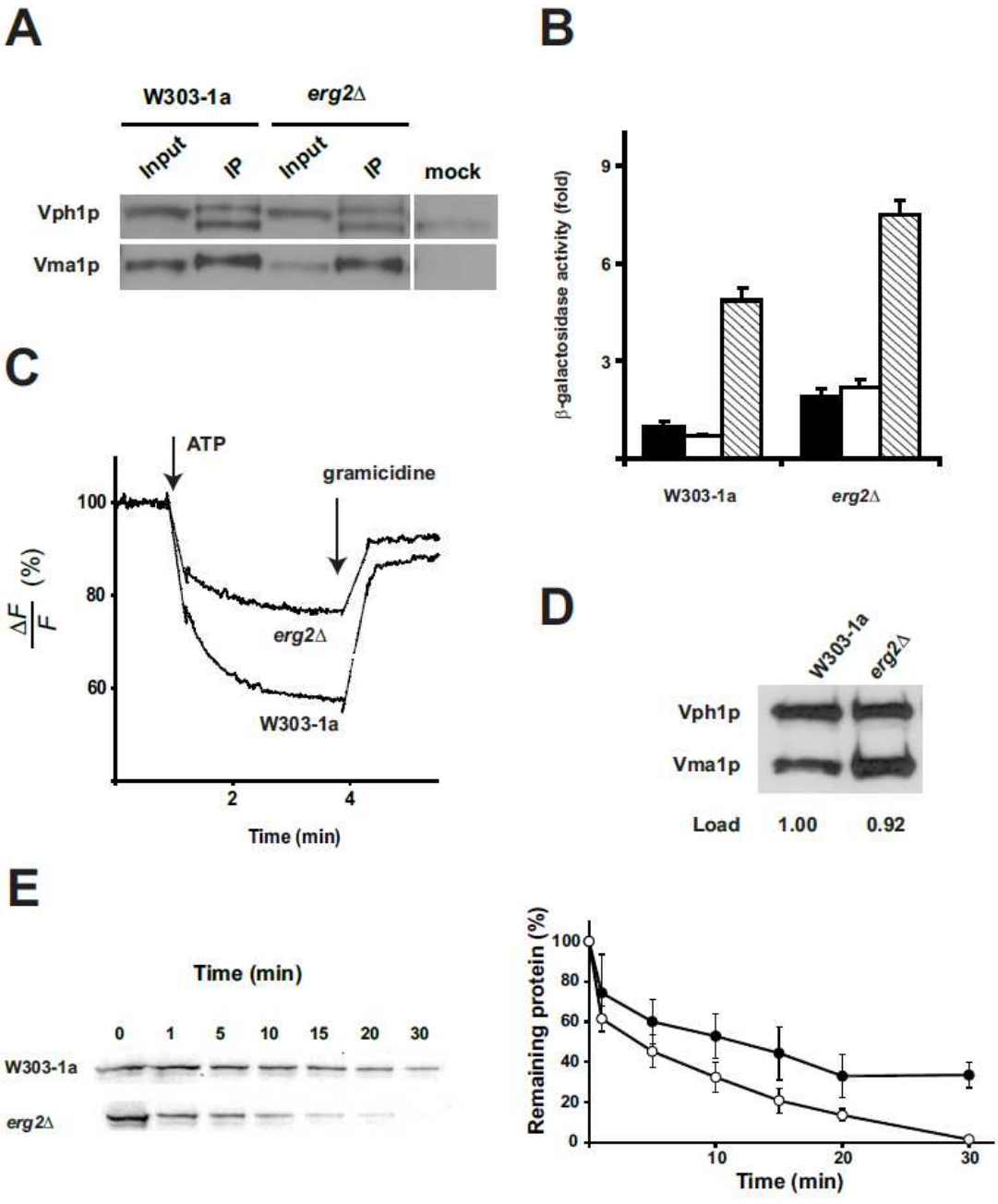

Figure 3
(Fitting 2 columns)

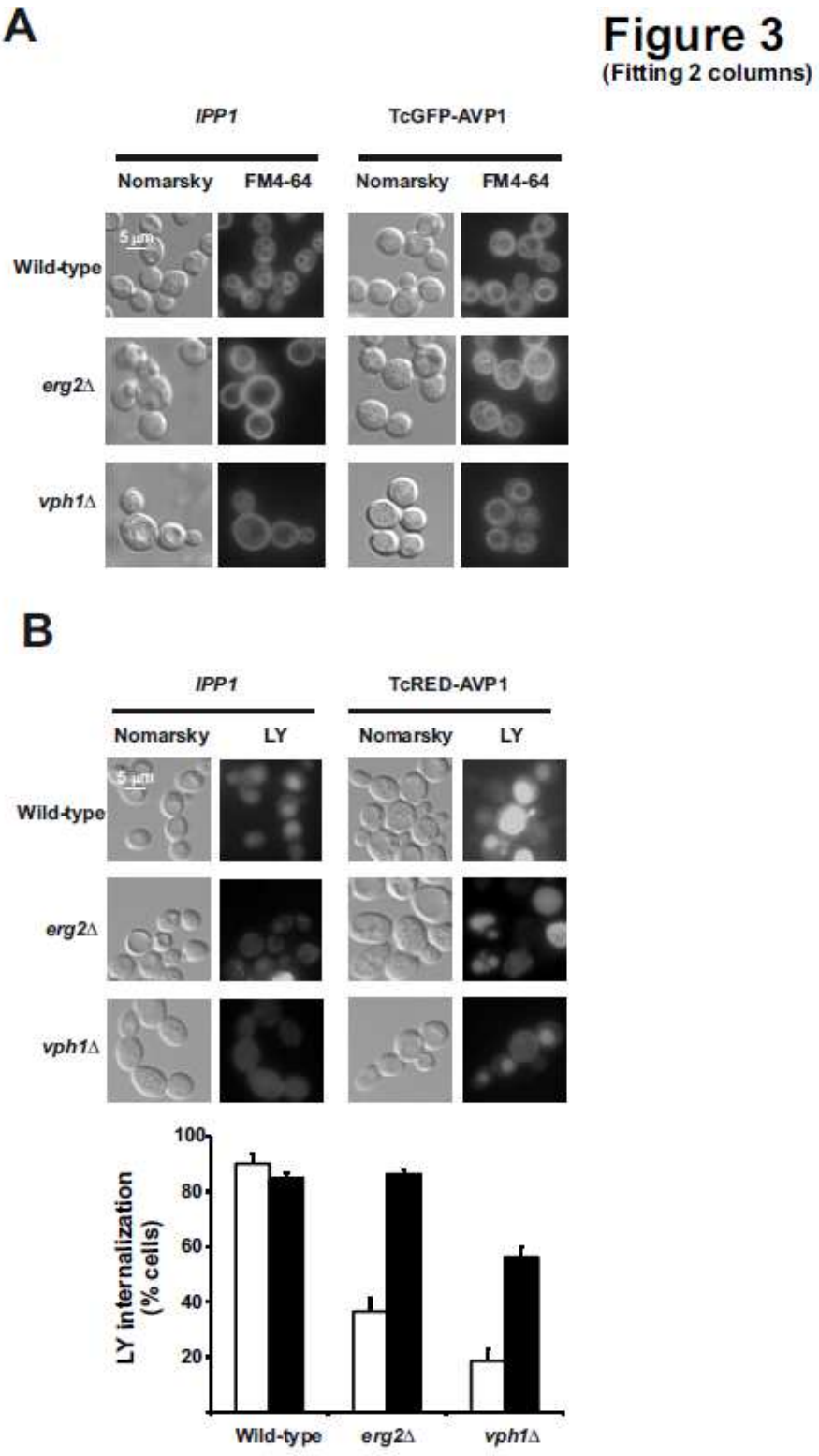

Figure 4

Fitting 1.5 columns

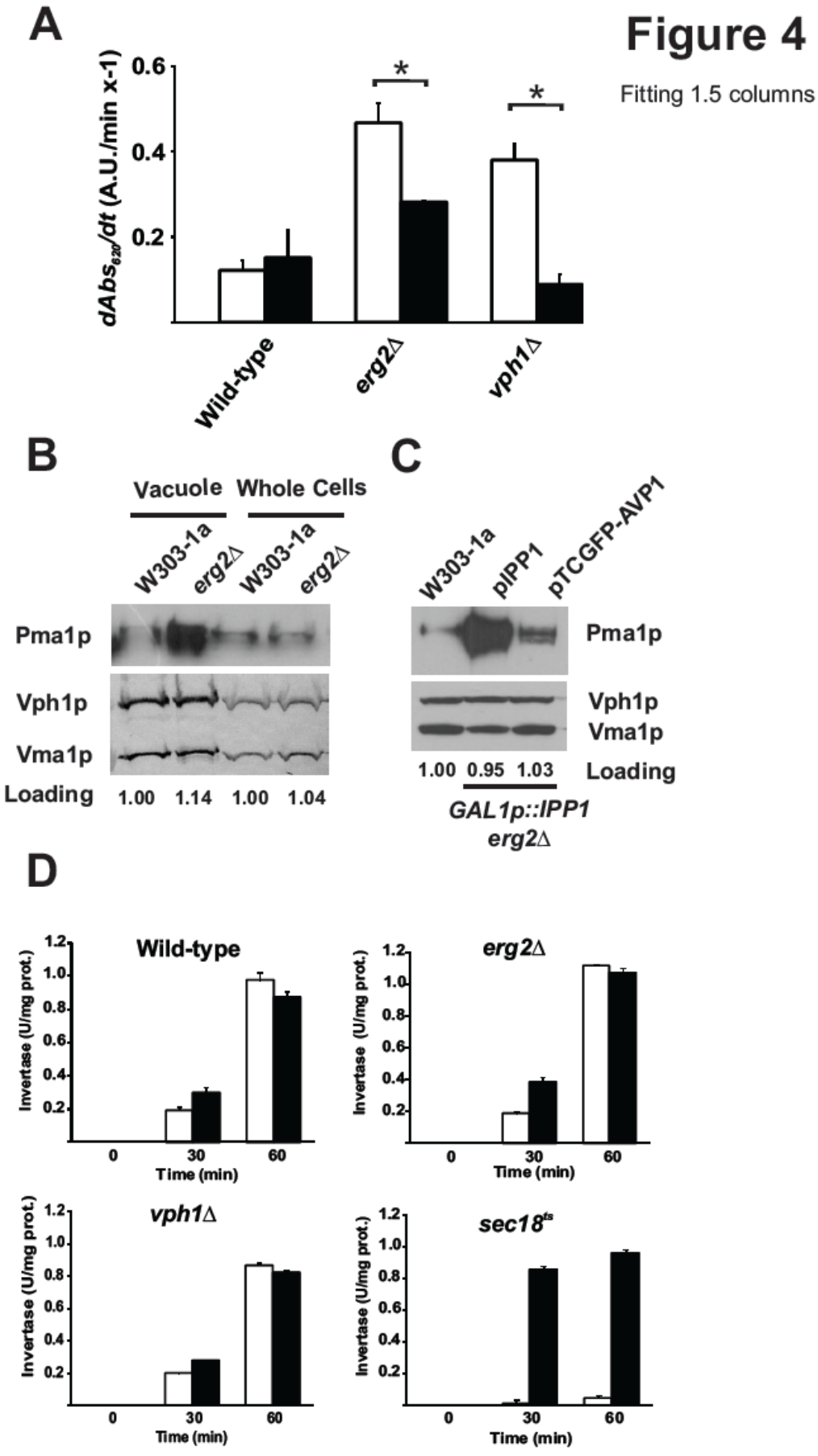

Figure 5
Fitting two columns

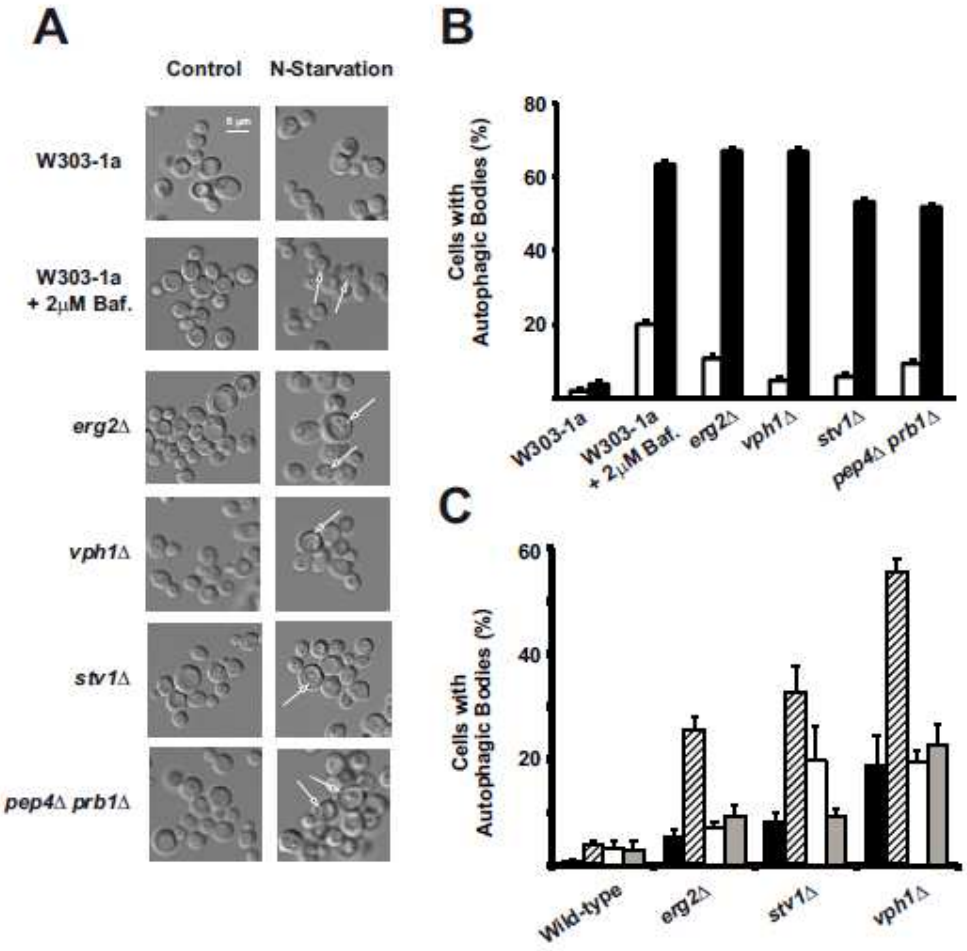

Figure 6
(Fitting 1.5 columns)

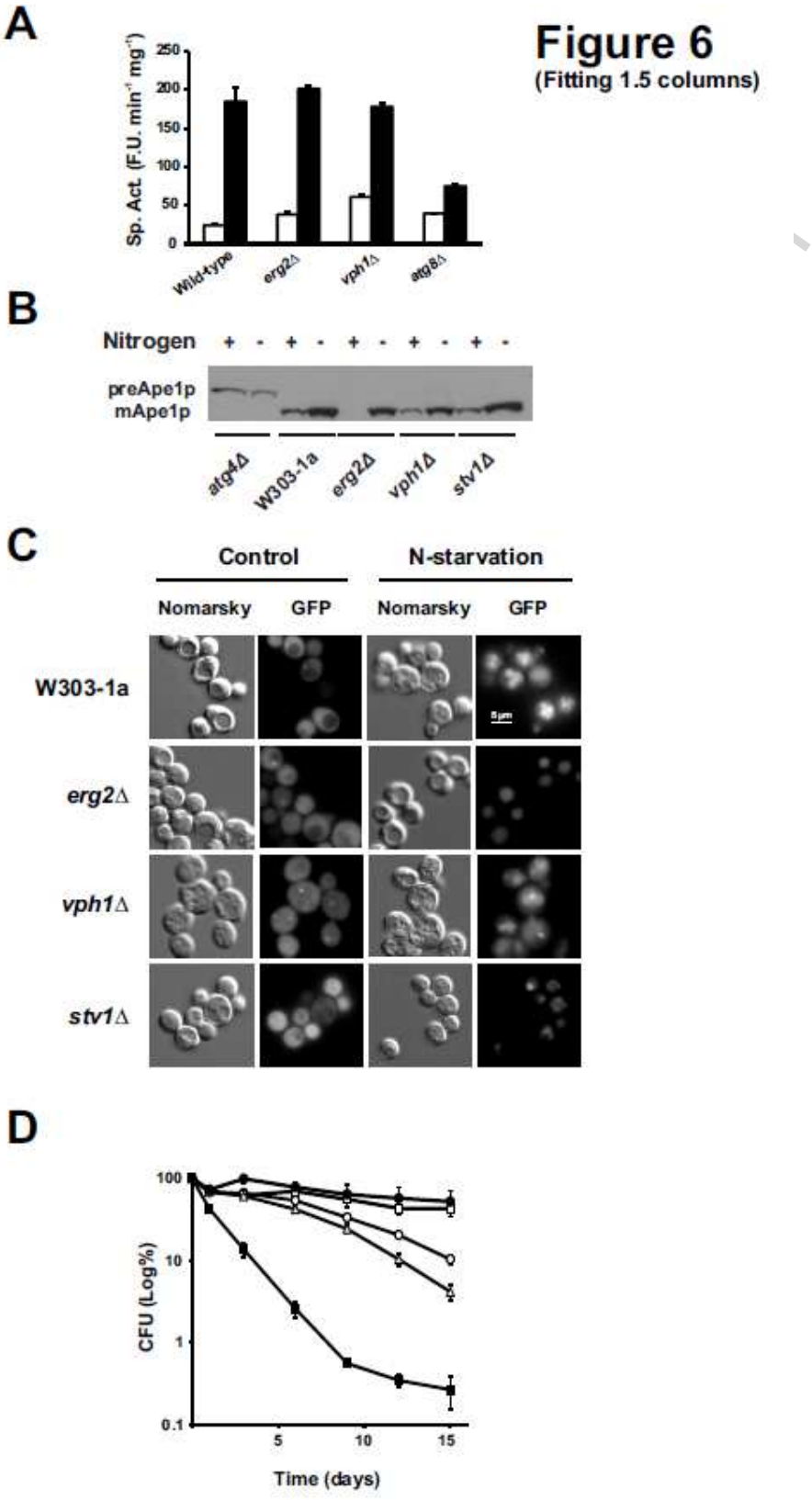

Figure 7
(Fitting 1 column)

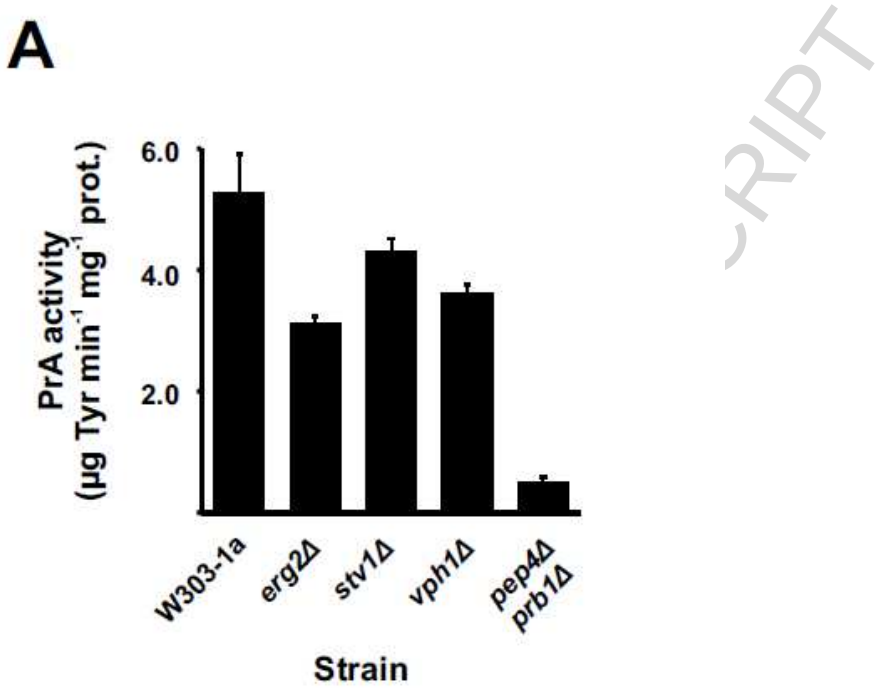

TABLES

Table 1. Yeast strains used in this work

Name	Relevant genotype	Reference
W303-1a	Mat a *leu2-3,112 trp1-1 can1-100 ura3-1 ade2-1 his3-11,15*	[68]
JRY7773	W303-1a *erg2Δ*::*TRP1*	[68]
JRY7775	W303-1a *erg3Δ*::*TRP1*	[68]
JRY7776	W303-1a *erg4Δ*::*TRP1*	[68]
RH6822	Mat a ura3 his3 leu2 bar1-1	[69]
RH6829	Mat a ura3 his3 leu2 trp1 bar1-1 erg5Δ::HIS5-GPD-DHCR24 erg6Δ::TRP1-GPD-DHCR7	[69]
SAH6	W303-1a *stv1Δ*::*TRP1*	This study
SAH7	W303-1a *vph1Δ*::*KanMX4*	This study
YPC3	W303-1a *ipp1$_{UAS}$-ipp1$_{TATA}$::HIS3-GAL1$_{UAS}$-GAL1$_{TATA}$-IPP1*	[39]
SAH2	YPC3 *erg2Δ*::*TRP1*	This study
SAH5	YPC3 *stv1Δ*::*TRP1*	This study
SAH6	YPC3 *vph1Δ*::KanMX4	This study
SEY6210	*Mat* α *his3-Δ200 leu2-3,112 lys2-801 trp1-Δ901 ura3-52 suc2-Δ9 GAL*	[70]
WPHYD7	SEY6210 *atg8Δ*::*LEU2*	[71]
UNY123	SEY6210 *atg4Δ*::*LEU2*	[72]
SAH27	SEY6210 GPD1promoter::*pho8Δ60::KanMX4*	This study
SAH18	W303-1a *erg2$_{UAS}$-erg2$_{TATA}$::KanMX4-GAL1$_{UAS}$-GAL1$_{TATA}$-ERG2*	This study
SAH23	SEY6210 *atg8Δ*::*LEU2* GPD1promoter::*pho8Δ60::KanMX4*	This study
SAH32	SEY6210 *vph1Δ*::*KanMX4* GPD1promoter::*pho8Δ60::natR*	This study
SAH33	SEY6210 *erg2Δ*::*KanMX4* GPD1promoter::*pho8Δ60::natR*	This study
SAH44	W303-1a GPD1promoter-GFP::*atg15::natR*	This study
SAH45	W303-1a *vph1Δ*::*KanMx4* GPD1promoter-GFP::*atg15::natR*	This study
SAH46	W303-1a *stv1Δ*::*TRP1* GPD1promoter-GFP::*atg15::natR*	This study
SAH47	SAH18 GPD1promoter-GFP::*atg15::natR*	
BJ3505	Mat a *pep4::HIS3 prb1-Δ1.6R lys2-208 trp1- Δ101 ura3-52 gal2 can*	[73]